Antiferromagnetism in Pr_3In

A. D. Christianson and J. M. Lawrence
University of California, Irvine, California 92697, USA

J. L. Zarestky
Ames Laboratory, Iowa State University, Ames, Iowa 50011, USA

H. S. Suzuki
National Institute for Materials Science, Tsukuba, 305-0047, Japan

J. D. Thompson, M. F. Hundley, and J. L. Sarrao
Los Alamos National Laboratory, Los Alamos, New Mexico 87545, USA

C. H. Booth
Lawrence Berkeley National Laboratory, Berkeley, California 94720, USA

D. Antonio and A. L. Cornelius
University of Nevada, Las Vegas, Nevada 89154, USA
(Received 18 November 2004; revised manuscript received 8 February 2005; published 1 July 2005)

We present neutron diffraction, magnetic susceptibility and specific heat data for a single-crystal sample of the cubic (Cu_3Au structure) compound Pr_3In. Antiferromagnetic order occurs below $T_N=12$ K with propagation vector $(0,0,0.5\pm\delta)$ where $\delta\approx 1/12$. The neutron diffraction results can be approximated with a model where the moments in each of the three Pr sublattices form ferromagnetic sheets perpendicular to and alternating in sign along the propagation direction, with a 12-unit-cell square-wave modulation. The very small specific heat anomaly that we observe at $T_N=12$ K may be a consequence of the fact that the ordered moment is *induced* in the Γ_1 singlet when $T<T_N$. The magnetic susceptibility indicates that in addition to the antiferromagnetic transition at 12 K, there may be a transition near 70 K below which there is a very small remnant magnetization ($0.005\mu_B$).

DOI: 10.1103/PhysRevB.72.024402 PACS number(s): 75.25.+z, 61.12.Ld, 75.30.Cr, 75.40.Cx

INTRODUCTION

The compound Pr_3In forms in the cubic Cu_3Au structure, the In atom sits at the origin and the Pr atoms at the face centers to form an ordered fcc structure. Previous work[1–3] on polycrystalline samples of this compound indicated the existence of an antiferromagnetic transition in the range 10–20 K. An additional ferromagnetic transition near 60 K was observed by some authors,[1,2] although others[3] argued that this transition was due to a secondary Pr_2In crystal phase. Although the Pr site symmetry is tetragonal, the crystalline electric field at the Pr site is believed to have nearly cubic symmetry[3,4] with a Γ_1 singlet ground state and a low-lying Γ_4 triplet excited state. The isostructural compound Pr_3Tl, for which similar statements hold, was studied extensively as a classic singlet-triplet induced moment ferromagnet.[4–7] In such systems, when the intersite exchange interaction is sufficiently large relative to the singlet-triplet splitting, a phase transition occurs such that for $T<T_C$ a moment is induced in the ground state singlet via admixture with the triplet states. Such induced order is also expected in Pr_3In.

In this paper, we report neutron diffraction, magnetic susceptibility and specific heat results for a single crystal of Pr_3In. We give a model of the antiferromagnetic structure which provides a good approximation to the diffraction data. Our specific heat data strengthens the case for singlet-triplet induced magnetism. We discuss the sample-dependence of the results, as well as the possible existence of a small ferromagnetic component of the structure.

EXPERIMENTAL DETAILS

A large (1 cm diameter by 2 cm long) cylindrical boule of Pr_3Tl was grown by the Bridgman technique using a Mo crucible. The neutron diffraction measurements were performed on the Ames Laboratory triple-axis spectrometer, HB1A, at the High Flux Isotope Reactor (HFIR) at the Oak Ridge National Laboratory (ORNL). The HB1A spectrometer operates with a fixed initial energy of 14.7 meV using a double pyrolitic graphite monochromator system. This, together with two HOPG filters, provides a very intense and clean neutron beam ($I_{\lambda/2}\sim 10^{-4}I_{\lambda}$). A pyrolitic graphite analyzer and collimations of 48′-40′-40′-102′ were also used. The sample contained a large (~ 1 cm^3) irregularly shaped crystallite that was not aligned with the growth axis of the boule, and several smaller crystallites. We performed measurements for both the (h,h,l) and $(h,k,0)$ reciprocal lattice planes of the large crystal oriented in the scattering plane of the spectrometer. Because of the large size and irregular shape and orientation of the crystal, we were unable to cor-

rect for extinction or for neutron absorption, which was significant due to the large absorption cross section of In. The units of intensity given below are counts per monitor count units (1 mcu$\approx$1 s); momentum transfer q is given in reduced units, i.e., in units of $2\pi/a_0$. The susceptibility and specific heat measurements were performed on two small pieces cut from the center of the boule; results of these measurements on the two pieces were identical. The susceptibility was measured in commercial (Quantum Design) SQUID magnetometers at Los Alamos National Laboratory (LANL) and Lawrence Berkeley National Laboratory (LBNL); the specific heat was measured via a thermal relaxation method using commercial (Quantum Design PPMS) systems at LANL and Las Vegas. The resistance was measured by a standard four-lead measurement.

EXPERIMENTAL RESULTS AND ANALYSIS

The low temperature neutron diffraction results confirmed the Cu_3Au crystal structure with lattice constant 4.94 Å. The inset to Fig. 1(c) displays the experimental structure factor $F^2_{\rm exp}=I\sin\theta$, i.e., the intensities multiplied by the Lorentz factor $\sin\theta$ appropriate for q-scans,[8] for several nuclear peaks in the $(1,-1,0)$ scattering plane. The upper solid line is the average value ($F^2_{\rm av}=13\,510$) of the experimental structure factor for the high intensity peaks; the lower solid line is the expected value $[13\,510\,[(b_{\rm Pr}-b_{\rm In})/(3b_{\rm Pr}+b_{\rm In})]^2=11]$ of the structure factor for the low-intensity peaks. The fact that the measured intensities of the low intensity peaks cluster around this latter value suggests that the Cu_3Au crystal structure is reasonably well ordered. The resistance ratio $RRR=R(300\ K)/R(4\ {\rm K})\sim 11$ measured for our sample supports this conclusion. The deviations from the expected values of $F^2_{\rm exp}$ arise primarily from (uncalculable) neutron absorption and extinction. Given these effects, it is not possible to rule out some degree of site disorder or variation of the stoichiometry from the 3:1 ratio.

The susceptibility, measured in a magnetic field of 0.01 T, is shown in Fig. 2. The peak at 12 K indicates the onset of antiferromagnetic order. The high temperature susceptibility [Fig. 2(a), inset] can be approximated by a Curie-Weiss law $\chi=C({\rm Pr})/(T+\theta)$ where $C({\rm Pr})=1.55$ emu/mol Pr is the free-ion Curie constant for Pr ($J=4$) and $\theta=-12$ K. The approximation is particularly good in the range 100–200 K; for $200<T<300$ K a better fit has $C=1.68$ emu/mol Pr and $\theta=+3$ K. A small jump occurs in the susceptibility at 70 K. This jump is seen more clearly in a plot of the effective moment $T\chi/C({\rm Pr})$, which approaches the free-ion value of unity at high temperature, but which increases to values greater than unity below 70 K [Fig. 2(b)]. This increase is a clear sign of a ferromagnetic contribution; the decrease at low temperatures arises both from saturation of the ferromagnetic contribution and from the onset of antiferromagnetism. Plots of the magnetization (Fig. 3) show hysteresis below 70 K. Both the coercive field (0.015 T) and the remanent magnetization ($0.005\mu_B$) are very small at $T=5$ K. Hence, the ferromagnetic contribution which occurs below 70 K is very weak in this compound.

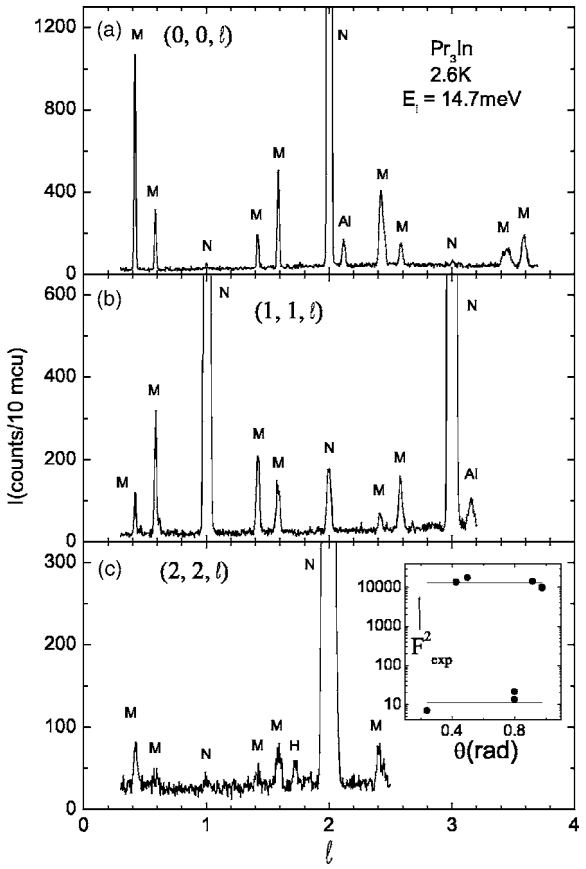

FIG. 1. Neutron diffraction profiles for Pr_3In at 2.6 K along three lines [(a) $[0,0,l]$; (b) $[1,1,l]$; and (c) $[2,2,l]$] in the $(1,-1,0)$ scattering plane. Peaks marked M are the primary magnetic reflections that appear below 12 K. Peaks marked N are nuclear reflections and peaks marked Al are due to polycrystalline aluminum in the beam. The peak marked H is a harmonic of the primary magnetic reflections. Inset, the experimental structure factor $I\sin\theta$ for the nuclear peaks in the $(1,-1,0)$ scattering plane. The upper solid line is the average value for the strong peaks; the lower solid line is the predicted value for the weak peaks based on the average value for the strong peaks. (mcu represents monitor count units.)

Figure 4 shows that the effect of increasing the magnetic field is to decrease the temperature of the susceptibility maximum [Fig. 4(a) and inset]. In the effective moment plots [Fig. 4(b) and inset] it can be seen that increasing the magnetic field decreases the magnitude of the discontinuity at 70 K. The susceptibility for a piece cut from the end of the Bridgman boule (and thus outside the region of the single crystallite used in the neutron measurement) is shown in both panels; the overall magnitude is similar to that of the centerpiece, but there is no sign of antiferromagnetic order. The resistance ratio ($RRR=5.5$) for the endpiece sample was a factor of 2 smaller than that of the sample cut from the center, hence the endpiece appears to be more disordered than the large crystallite.

The specific heat data is shown in Fig. 5. The lattice contribution was determined from previous measurements[9] of La_3In; the temperature-dependent Debye temperature $\Theta_D(T)$ given in that paper was extrapolated in linear fashion to higher temperature ($T>16$ K) and then used to evaluate the

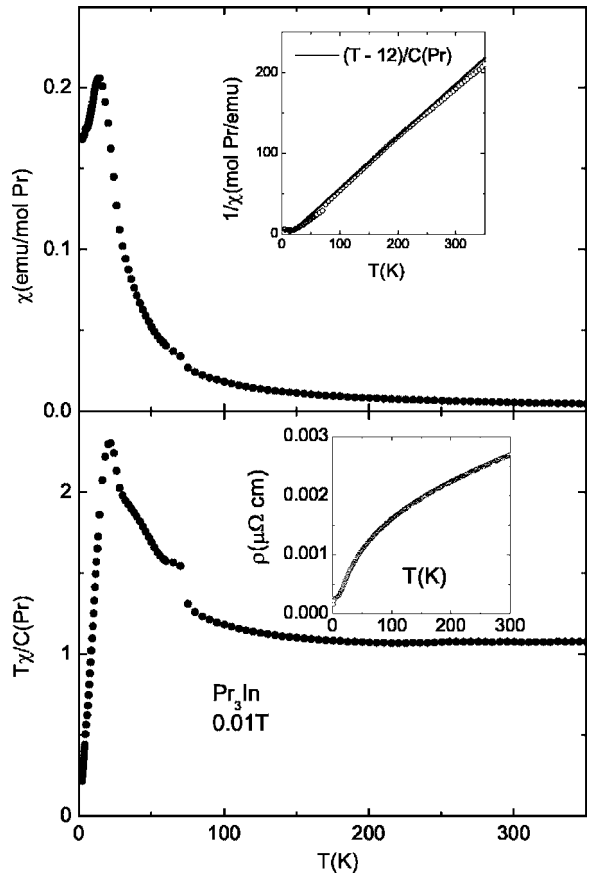

FIG. 2. (a) The susceptibility $\chi(T)$ of Pr_3In measured with $H=0.01$ T for a piece cut from the center of the single crystal. The inset compares the inverse susceptibility to a Curie-Weiss law. (b) The effective moment $T_\chi/C(\mathrm{Pr})$ where $C(\mathrm{Pr})$ is the Pr free-ion Curie constant. Inset: The resistivity.

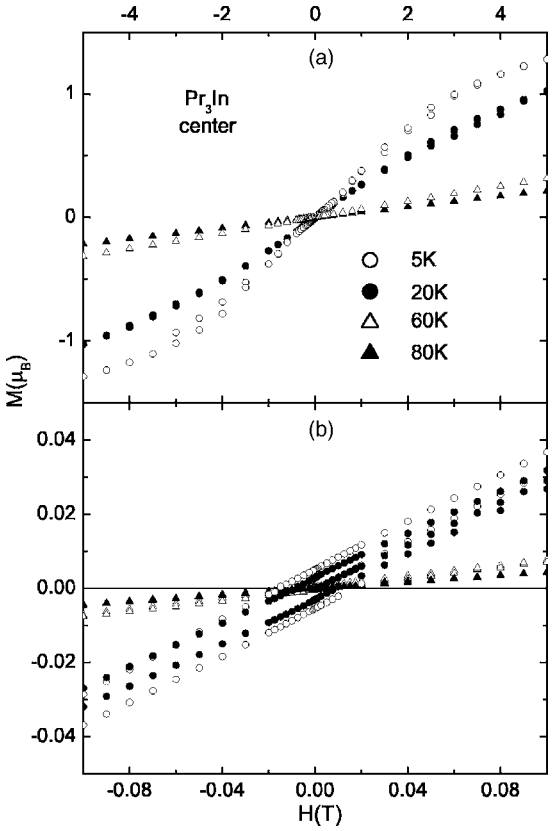

FIG. 3. (a) The magnetization of Pr_3In at four temperatures above and below the transition at 70 K. Data taken with both field increasing and field decreasing are included to establish the hysteresis that occurs below 70 K. (b) Magnetization shown on an expanded scale.

Debye specific heat. The magnetic specific heat $C_{\mathrm{mag}}(T)$ then was taken as the measured value minus the lattice contribution. The upturn in $C_{\mathrm{mag}}(T)/T$ at the lowest temperatures [Fig. 5(b), inset] is from a contribution of the Pr nucleus due to a large hyperfine field, in agreement with Ref. 3. The magnetic specific heat and the corresponding entropy is very small at 12 K and the specific heat anomaly associated with the antiferromagnetic transition is so weak as to be only barely visible in a plot of C_{mag}/T [Fig. 5, inset]. No sign of an anomaly in the specific heat was observed near 70 K, where the susceptibility exhibits a discontinuity.

Figure 1 shows the magnetic reflections (marked M) observed below 12 K in the neutron diffraction for the $(1,-1,0)$ scattering plane. Strong [e.g., (0, 0, 2)] and weak [e.g., (1, 1, 2)] nuclear reflections (marked N) are also present, as well as peaks (marked Al) arising from polycrystalline aluminum in the sample environment. The magnetic peaks can be indexed as occurring at $q=(h,k,l+\frac{1}{2}\pm\delta)$ where $\delta=0.083\approx 1/12$. (We cannot rule out that the ordering is slightly incommensurate.) Similar results were seen in the (0, 0, 1) scattering plane, where peaks were observed at $(h+\frac{1}{2}\pm\delta,k,0)$ and $(h,k+\frac{1}{2}\pm\delta,0)$. In addition to these primary reflections, several 3δ harmonics were observed, e.g., the peak marked H at (2, 2, 1.75) seen in Fig. 1(c). Finally, a single 4δ harmonic was observed at (1, 1.16, 0). The primary magnetic peaks and the 3δ and 4δ harmonics vanish above 12 K and the temperature dependence of the 1δ, 3δ, and 4δ reflections can be approximated as $B_i+C_i[(T_N-T)/T_N]^{1/2}$ where $T_N=11.4$ K but where the backgrounds B_i and coefficients C_i are different for the different reflections (Fig. 6). Hence the harmonics have the same temperature dependence as the order parameter, which varies in a manner typical of an antiferromagnetic transition. In addition, there may be a small variation in the value of the ordering wave vector, i.e., δ, between 10 and 12 K [Fig. 6(b), inset], suggesting that the wave vector is initially incommensurate, but then locks on to the commensurate value 1/12 below 10 K.

The magnetic line intensities observed in Fig. 1 can be approximated by the following model (Fig. 7, insets). Each of the three Pr sites in the unit cell $[r_1=(\frac{1}{2},\frac{1}{2},0)$, $r_2=(0,\frac{1}{2},\frac{1}{2})$, and $r_3=(\frac{1}{2},1,\frac{1}{2})]$ gives rise to a sublattice $[r_i+(h,k,l)]$ of spins consisting of ferromagnetic sheets perpendicular to the propagation (z) direction where the direction of the moments alternate in sign when $l\rightarrow l+1$. In and of itself this would yield a basic two-unit cell structure with $q=(0,0,\frac{1}{2})$. The direction of the moments is, however, further modulated by a 12-unit-cell square wave so that the magnetic reflections occur at $q_z=\frac{1}{2}\pm(2n+1)\delta$, where $\delta=1/12$. In Fig. 7, the direction of the moments in the first unit cell is taken

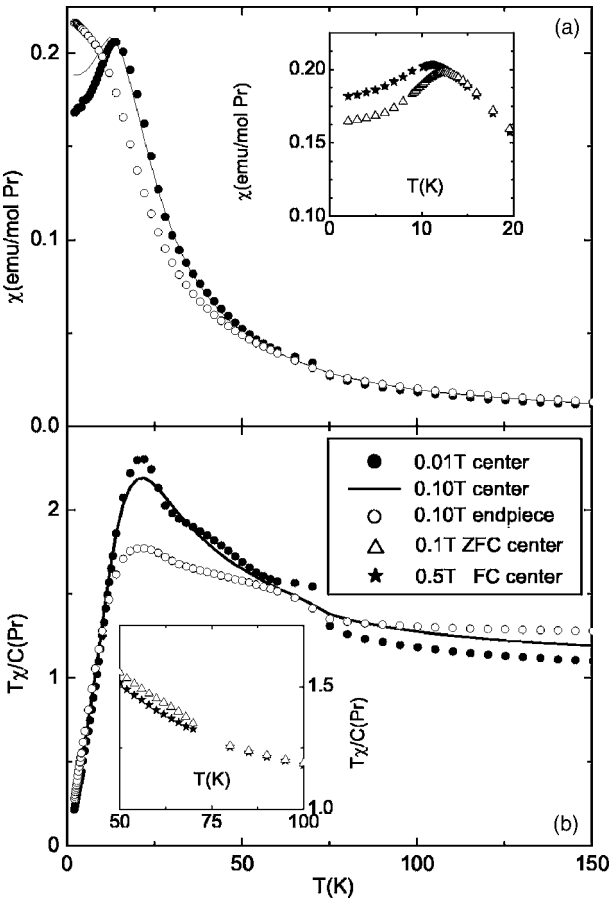

FIG. 4. (a) The susceptibility at $H=0.01$ and 0.1 T for a piece cut from the center of the single crystal of Pr_3In together with susceptibility for a piece cut from the end of the Bridgman boule. The inset emphasizes the effect of increasing magnetic field on the susceptibility near the antiferromagnetic transition. (b) The effective moment $T_\chi/C(\mathrm{Pr})$ under the same conditions as in (a); the inset emphasizes the effect of increasing magnetic field on the susceptibility near the transition at 70 K.

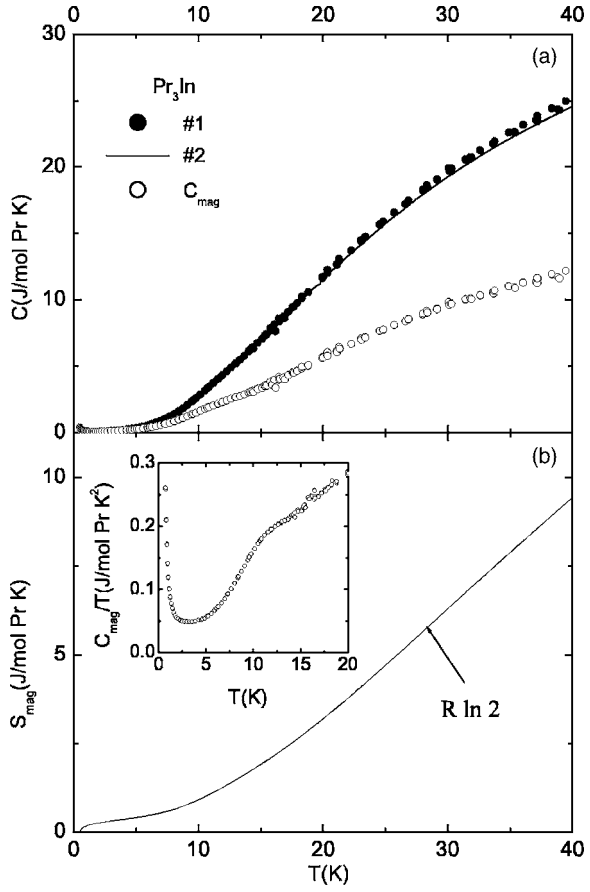

FIG. 5. (a) The specific heat for two samples cut from the center of the single crystal of Pr_3In. The open circles exhibit the magnetic contribution, determined as discussed in the text. (b) The entropy associated with the magnetic specific heat. The inset shows the linear coefficient $C_{\mathrm{mag}}(T)/T$.

as $\hat{S}_1=(1,0,0)$, $\hat{S}_2=(-1/2,0,-\sqrt{3}/2)$, and $\hat{S}_3=(-1/2,0,+\sqrt{3}/2)$; but other alignments of spins [e.g., $\hat{S}_1=(1,0,0)$, $\hat{S}_2=(0,1,0)$, and $\hat{S}_3=(0,0,1)$] such that $S_{1xy}=(S_2+S_3)_{xy}$, give essentially similar results. The magnitude of the Pr moments is $1\mu_B$; variation of $(S_2+S_3)_{xy}$ away from the value $1\mu_B$ significantly degrades the comparison to experiment. The results of a calculation of the diffraction intensities for this structure are compared to the measured magnetic reflection intensities in Fig. 7. The calculated intensities have been normalized to the experimental nuclear structure factor [Fig. 1(c), inset] to facilitate direct comparison to the experimental data. The intensities are modulated as a function of angle by the Pr form factor and the Lorentz factor, taken again as $\sin\theta$. Figure 7 shows that this model gives a good first approximation to the line intensities. It reproduces the alternation of intensities along and between $[h,h,l]$ lines and it approximates the magnitudes fairly well. Some of the predicted harmonics [e.g. (2, 2, 1.75)] are observed at about the correct intensity.

DISCUSSION

We first consider the role of sample quality on these results. As mentioned above, given the uncertainties due to absorption and extinction, we cannot rule out some degree of disorder or deviation from the correct 3:1 stoichiometry. Given that Pr_3In is slightly peritectic,[10] i.e., it does not grow congruently from the melt, it is reasonable to assume that samples grown as arc-melted polycrystals or as Bridgman-grown single crystals will deviate somewhat from the correct 3:1 stoichiometry. This is probably the main source of disagreement between results reported here and in earlier studies[1–3] on different samples. We note that the susceptibility of a piece cut from the end of our sample (Fig. 4) shows no antiferromagnetic transition, which probably results from a stoichiometry variation between the outer edges and the center of the boule, where the large single crystal was located.

We stress that while all previous studies were performed on polycrystalline samples, for which careful metallography indicated the presence of second phases,[3] the work reported here was performed on a single crystal. The resistance ratio $RRR=11$ measured for our sample (Fig. 2b, inset) is twice as large as that reported in Ref. 2, indicating that our sample is

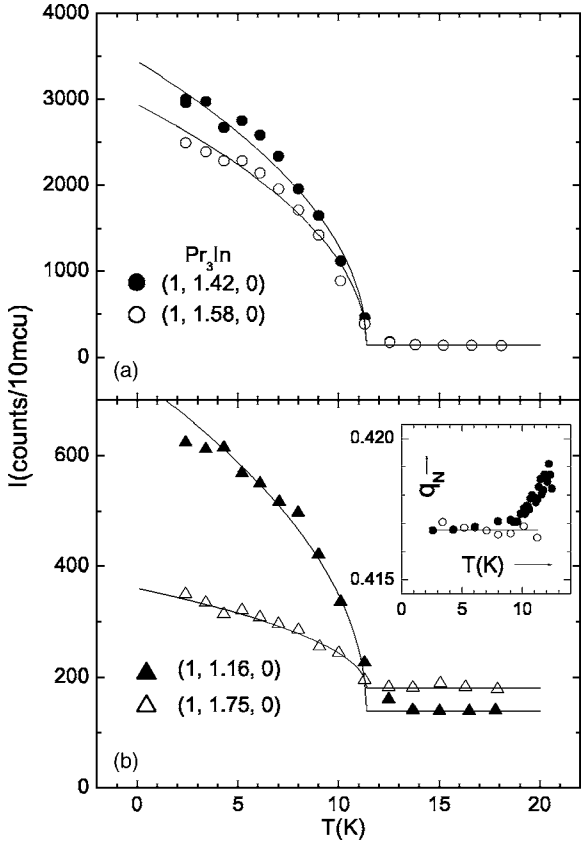

FIG. 6. The intensity in the primary magnetic reflections (1, 1.42, 0) and (1, 1.58, 0) (a) and in the 4δ (1, 1.16, 0) and 3δ (1, 1.75, 0) harmonics (b) vs temperature. The solid lines represent the behavior $B_i + C_i[(T_N - T)/T_N]^{1/2}$ with $T_N = 11.4$ K and with B_i and C_i varying between reflections. (mcu represents monitor count units.)

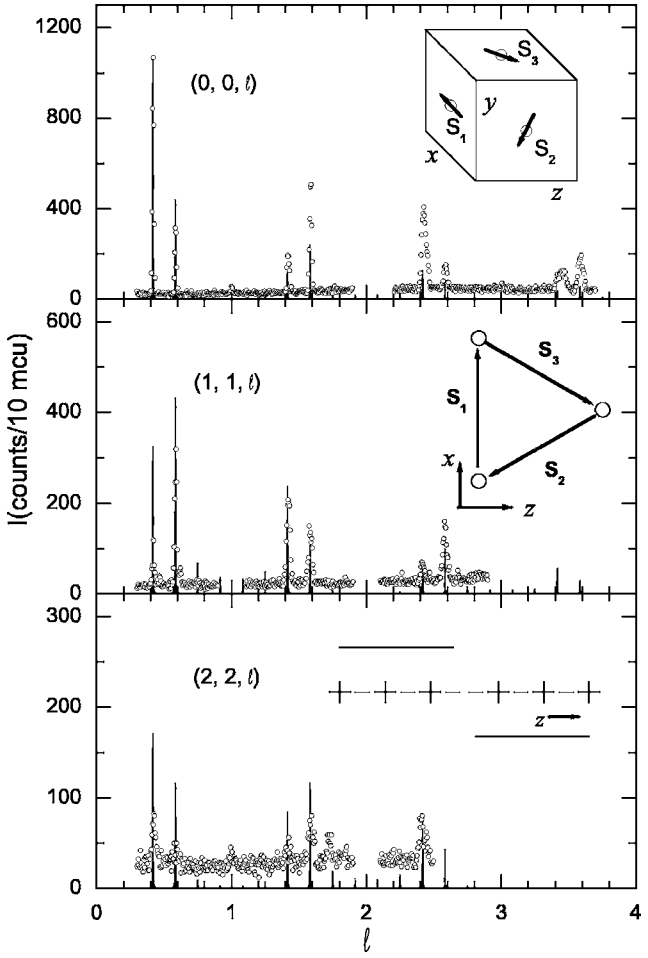

FIG. 7. The measured magnetic reflections (open circles) compared to the intensities calculated for the model of the antiferromagnetic order given in the text (solid lines). The insets depict the model: (a) Three Pr moments S_i of magnitude $1\mu_B$ sit on the face centers of the unit cell; (b) the moments lie in the xz plane at angle 120° with respect to each other and sum to zero as shown; (c) each S_i forms a sublattice that consists of ferromagnetic sheets in the xy plane that alternate in sign along the z direction within the envelope of a 12-unit cell square wave. (mcu represents monitor count units.)

better ordered. In addition, the inset to Fig. 1(c) shows that the intensities of the weak nuclear lines (those that are forbidden in the disordered fcc structure) have roughly the right magnitude relative to the strong lines as to suggest a reasonably well-ordered Cu_3Au structure. While past studies of Pr_3In (Refs. 1–3) show variation in the transition temperature and magnitude of the antiferromagnetic peak in the susceptibility, the *existence* of the antiferromagnetic transition is clearly intrinsic. Given these circumstances, we believe that the magnetic reflections seen in the neutron diffraction measurement are essentially those of well-ordered Pr_3In. The transition temperature T_N, the wavelength of the square wave modulation, and the magnitude of the ordered moment might be affected somewhat by sample quality, but the basic structure should be unaffected.

Considerable variation also has been observed in the transition temperature and magnitude of the ferromagnetic anomaly in the susceptibility near 60–70 K.[1–3] In our samples the anomaly is smaller than that seen in other studies, with the exception of Ref. 3, where no such anomaly was seen. However, the field used in the latter study (1.5 T) was sufficiently large that (given the field dependence shown here in Fig. 4) the anomaly may have been suppressed. Our neutron diffraction results provide no indication of the presence of a Pr_2In phase, which was implicated by Ref. 3 as the origin of the anomaly. However, the extremely small remnant magnetization makes it difficult to understand the origin of this transition if it is intrinsic.

The very small anomaly that we observe in the specific heat at the antiferromagnetic transition was also reported in Ref. 3. This effect is quite striking, especially given the well-defined temperature dependence of the order parameter, which is typical for an antiferromagnetic transition. In an early study[4] of the classic singlet-triplet ferromagnet Pr_3Tl, a negligible specific heat anomaly was also observed near the ferromagnetic transition at $T_C = 11.3$ K. This was attributed to the fact that in a mean-field treatment of the induced-moment ferromagnet, there is no change in entropy in the Γ_1 singlet at the transition, but rather the singlet, which has no moment above T_C, acquires a moment from admixture with the Γ_4 states below T_C. In any case, the similarities between Pr_3In and Pr_3Tl—in the Cu_3Au crystal structures, the transition temperatures $T_N \approx T_C \approx 11-12$ K, and in the weak spe-

cific heat anomaly—suggest that the antiferromagnetism in the former compound is induced in a Γ_1 singlet, as is the ferromagnetism in the latter compound.

Turning now to the magnetic structure, we note that models where the two spins in the base unit cell at $z=\frac{1}{2}$ have total projection onto the (0, 0, 1) plane equal to that of the ($\frac{1}{2}$, $\frac{1}{2}$, 0) spin give good fits to the magnetic reflection intensities. For the model shown in Fig. 7, the three spins in the unit cell point along the edges of an equilateral triangle, and therefore sum to zero. This is the lowest energy state for the simpler case of three antiferromagnetically coupled spins on an equilateral triangle.[11] In the present case, ferromagnetic next-nearest-neighbor (NNN) interactions must be present to stabilize the ferromagnetic sublattices of these three nearest neighbor (NN) spins. However, were there only antiferromagnetic NN and ferromagnetic NNN interactions, the lowest state would be a $q=0$ structure with all unit cells identical to the core cell. The complicated structure that we observe, with the sign of the moments alternating between neighbor cells along the propagation direction, and further modulated by the 12-unit-cell square wave, requires longer range interactions.

For several reasons, this model is only a first approximation to the antiferromagnetic structure. First, the predicted line intensities do not agree perfectly with the data. To an unknown extent, the discrepancies can be attributed to the same sources as the deviations seen in Fig. 1(c), inset, in particular the uncalculable absorption and extinction corrections. Second, in this structure no even harmonics are expected, whereas a 4δ harmonic was observed at (1, 1.16, 0) with a temperature dependence (Fig. 6) proportional to the order parameter. Finally, the susceptibility suggests that there may be a ferromagnetic component in the structure which may reflect a small canting of the moments, giving a ferrimagnetic component to the order. Given the small remnant magnetization $0.005\mu_B$ deduced from Fig. 3, the effects of this component on the line intensities are not resolvable in the present experiment. Despite all this, we believe that our model captures the essence of the antiferromagnetic order in Pr_3In.

CONCLUSION

We have shown that antiferromagnetic order with primary reflections at $q=\left(h,k,l+\frac{1}{2}\pm 0.083\right)$ occurs below 12 K in Pr_3In. There is very little entropy change associated with the transition and we argue that the physics involves singlet-triplet induced moment magnetism. In addition, a weak ferromagnetic component may set in near 70 K. Further experiments are needed to determine the sample dependence of the behavior, and to refine the magnetic structure. The crystal-field level structure needs to be determined directly by neutron scattering to prove that the singlet-triplet Γ_1/Γ_4 model is applicable. Finally, given that the soft dispersive crystal field modes expected near the transition in the singlet-triplet model have not been observed experimentally, even in the simpler ferromagnetic case of Pr_3Tl,[6,7]measurement of the spin dynamics is a crucial future experiment.

ACKNOWLEDGMENTS

The authors thank Steve Shapiro, Eric Bauer, and Jason Gardner for helpful discussions. Work at UC Irvine was supported by the U. S. Department of Energy (DOE) under Grant No. DE-FG03-03ER46036. Work at UNLV was supported by DOE EPSCoR-State/National Laboratory Partnership Grant No. DE-FG02-00ER45835 and Cooperative Agreement Grant No. DE-FC08-01NV14049. Work at LBNL was supported by the Director, Office of Science, Office of Basic Energy Sciences, of the U.S. DOE under Contract No. DE-AC03-76SF00098. Ames Laboratory is operated by Iowa State University for the U.S. Department of Energy (DOE) under Contract No. W-7405-ENG-82. Work performed at the HFIR Center for Neutron Scattering was supported by the DOE Office of Basic Energy Sciences Materials Science, under Contract No. DE-AC05-000R22725 with UT-Battelle, LLC. Work at Los Alamos was performed under the auspices of the DOE.

[1] B. Stalinski, A. Czopnik, N. Iliew, and T. Mydlarz, Phys. Status Solidi A **19**, K161 (1973).
[2] C. S. Garde and J. Ray, J. Magn. Magn. Mater. **189**, 293 (1998).
[3] F. Heiniger, E. Bucher, J. P. Maita, and LK. D. Longinotti, Phys. Rev. B **12**, 1778 (1975).
[4] K. Andres, E. Bucher, S. Darack, and J. P. Maita, Phys. Rev. B **6**, 2716 (1972).
[5] P. Bossard, S. Bakanowski, J. E. Crow, T. Mihalisin, and W. J. L. Bowers, J. Appl. Phys. **50**, 1892 (1979).
[6] R. J. Birgeneau, J. Als-Nielsen, and E. Bucher, Phys. Rev. B **6**, 2724 (1972).
[7] W. J. L. Buyers, T. M. Holden, and A. Perreault, Phys. Rev. B **11**, 266 (1975).
[8] R. Pynn, Acta Crystallogr., Sect. B: Struct. Crystallogr. Cryst. Chem. **B31**, 2555 (1975).
[9] F. Heiniger, E. Bucher, J. P. Maita, and P. Descouts, Phys. Rev. B **8**, 3194 (1973).
[10] *Binary Alloy Phase Diagrams*, 2nd ed., edited by T. B. Massalski, H. Okamoto, P. R. Subramanian, and L. Kacprzak (ASM International, Materials Park, OH, 1990), Vol. 3, p. 2275.
[11] R. Moessner, Can. J. Phys. **79**, 1283 (2001).